Active Flutter Suppression in a 2-D Airfoil Using Linear Matrix Inequalities Techniques

Samuel da Silva
samsilva@fem.unicamp.br
Department of Mechanical Design
State University of Campinas – UNICAMP
Rua Mendeleiev s/n, Cidade Universitária
13083-970 Campinas, SP, Brazil

Vicente L. Júnior
Emeritus Member, ABCM
vicente@dem.feis.unesp.br
Department of Mechanical Engineering
Universidade Estadual Paulista – UNESP
Av. Brasil, n.º 56, Centro
15385-000 Ilha Solteira, SP, Brazil

Flutter is an in-flight vibration of flexible structures caused by energy in the airstream absorbed by the lifting surface. This aeroelastic phenomenon is a problem of considerable interest in the aeronautic industry, because flutter is a potentially destructive instability resulting from an interaction between aerodynamic, inertial, and elastic forces. To overcome this effect, it is possible to use passive or active methodologies, but passive control adds mass to the structure and it is, therefore, undesirable. Thus, in this paper, the goal is to use linear matrix inequalities (LMIs) techniques to design an active state-feedback control to suppress flutter. Due to unmeasurable aerodynamic-lag states, one needs to use a dynamic observer. So, LMIs also were applied to design a state-estimator. The simulated model consists of a classical flat plate in a two-dimensional flow. Two regulators were designed, the first one is a non-robust design for parametric variation and the second one is a robust control design, both designed by using LMIs. The parametric uncertainties are modeled through polytopic uncertainties. The paper concludes with numerical simulations for each controller. The open-loop and closed-loop responses are also compared and the results show the flutter suppression. The perfomance for both controllers are compared and discussed.
***Keywords**: Flutter, active control, LMI, polytopic uncertainties, robustness*

Introduction

Flutter occurs when the fluid surrounding a structure feeds back dynamic energy into the structure instead of absorbing it. Typically a structure will be stable up to a limiting velocity (the flutter velocity) for given conditions. Flutter is more likely to occur in wings, ailerons and other flexible parts of aircrafts with considerable aerodynamic loads. This aeroelastic phenomenon can cause increasing wing fatigue and limit aircraft flight velocities. So, it is necessary in the aeronautic industry to reduce or to suppress this effect, (Bisplinghoff et al., 1996).

In the last decades, this problem has been studied by many authors using different techniques. De Marqui Jr et al. (2001) conducted a complete historical review of flutter, showing the main methodologies and developments to suppress flutter in aircraft. In general, one can use either passive or active techniques.

Passive flutter supression techniques add weight to change the local or global stiffening and require redesign. Components can also be moved to perform a mass balancing, but this methodology may be not feasible in some situations. Another strategy is to operate below the flutter velocity, but this procedure reduces flight perfomance.

On the other hand, active flutter suppression control system suppresses flutter without redesign and adding mass. The idea is old and it was first tested in 1973 on a B-52-E aircraft that achieved flight velocity above the specified limit, besides some problems with model accuracy and robustness, (Garrick, 1976).

Nowadays, there are many control techniques that can be used for active flutter control. For instance, Olds (1997) used a flat plate in a 2-D flow and numerically simulated the uncontrolled model using Matlab®. Linear Quadratic Regulator (LQR) theory was used to design a state-feedback controller to maintain stability of the closed loop system at the flutter velocity. Despite good perfomance, the results are unrealistic because LQR controller requires all states to be known at all times in order to use state feedback. In real applications, it is not reasonable to expect that all states used are available.

Bail (1997), considering the same model of Olds (1997), used state estimators for compensate the lack of information. He investigated and compared two control methods by using a dynamic observer, namely the LQG control and H_∞ control, solved by Ricatti equations. Bail (1997) considered the disturbance-rejection problem assuming the external disturbance modeled by a wind gust in a control-flap. Norlander et al. (2000) also used simple LQG control techniques to evaluate a model on a wind-tunnel test. Haley and Soloway (1996) have made an experimental investigation in a transonic wind-tunnel to demonstrate the use of the generalized predictive control for flutter suppression of a subsonic airfoil.

Non-conventional techniques can also be used to suppress flutter. Belo et al. (2001) described an investigation on the application of fuzzy logic by using the method of Mamdani to establish control laws for flutter suppression. They simulated an aerolastic structure (NACA 0012 type rigid rectangular wing) with two-dimensional and non-linear aerodynamic behavior. However, non-conventional techniques, in special those based in fuzzy logic and neural networks, are not well defined in terms of passivity, robustness and stability. Many papers employ non-conventional techniques, but many omit stability and robustness proofs. Several researchers have studied these topics and managed to prove stability and robustness characteristics in this kind of controller. The development in this area is recent, (Lewis, 1999).

One of the most recent developments in active control uses convex optimization algorithms to solve problems described by linear matrix inequalities (LMI) requirements, (Ghaoui and Niculescu, 2000). There are many toolbox codes specially developed to solve this kind of problem, for example, LMI Toolbox Matlab®, (Gahinet et al., 1995) and LMISol®, with free code, (Oliveira et al., 1997). Once formulated in terms of an LMI, a problem can be solved efficiently through these algorithms, (Gahinet et al., 1995).

The LMI approaches contributed to overcome many difficulties in control design. In the last decade, LMI technique has been used to solve many problems that were unfeasible with other methodologies, (Boyd et al. 1994). The major advantage of LMI design is to enable specifications such as stability requirements, decay rate, input force limitation in the actuators and output peak bounder, (Silva et al., 2004). LMI also permits the consideration of

Paper accepted October, 2005. Technical Editor: José Roberto de F. Arruda.

model parameter uncertainties. It is a very useful tool for problems with constraints, where the parameters vary over a range of values.

Thus, the main aim of this article is to present a methodology for active flutter suppression with robustness to parametric uncertainties, based on LMI techniques. Harman and Liu (2002) demonstrated that it is necessary to consider robustness in flight control design. They have shown some typical reasons: a large envelope flight operation requires the controller to be robust (in combination with gain scheduling techniques); fly-by-wire control tends to provide poor handling quality; aircraft agility (e.g. rapid maneuver) requires robustness when the aerodynamic control is lost; and in hypersonic flight, high speed requires stability robustness as well. Harman and Liu discussed some popular control techniques in robust flight control applications and one of these is the possible application of LMI techniques (classified by the authors as *postmodern control*).

The present paper considers a linear system with polytopic uncertainty in some parameters of the system. The control procedure using LMI with polytopic uncertainty was first proposed by Geromel et al. (1991). The same model simulated by Bail (1997) and Olds (1997) is used. The paper is devoted to active flutter-supression by using LMI frameworks, so, the aerodynamic model is not discussed in detail. Two regulators were designed, the first one is a non-robust design for parametric variation and the second one is a robust control design. The numerical application compares the open-loop and closed-loop responses of each controller. The results show the flutter suppression obtained with the present methodology. The perfomance of both controllers are compared and discussed. Finally, conclusions are presented together with some future research directions for active flutter suppression by using LMI frameworks.

Nomenclature

A = dynamic matrix
A_{ai} = aerodynamic-lag states (i = 1,…,4)
b = semichord
B = input matrix
c = distance of control flap from shear center
C = output matrix
h = position with respect to plunge
I_α = moment of inertia of pitch angle
I_β = moment of inertia of flap angle
K = stiffness matrix
K_α = stiffness of pitch spring
K_β = stiffness of flap spring
K_h = stiffness of plunge
K_c = controller gain matrix
K_e = observer gain matrix
l = distance to trailing-edge flap center of gravity from c
L = lift
L_1 = lift per unit span on main section
L_2 = lift per unit span on trailing-edge control surface
m = mass of airfoil
m_1 = mass of main body
m_2 = mass of trailing-edge control surface
M = moment of external forces
M_1 = pitching moment on main section
M_2 = pitching moment on trailing-edge flap
M_a = mass matrix
S = static moment
S_α = static moment of pitch angle
S_β = static moment of flap angle
T = torque of flap spring
u = input control
V = velocity
V_f = flutter velocity
x = state vector
y = output vector

Greek Symbols

α = *pitch angle*
β = *flap angle*
ρ = *air density*
μ = *controller decay rate*
γ = *observer decay rate.*
σ = *maximum value of input control amplitude*
Ω = *convex space*

A Two-Dimensional Aeroelastic Airfoil Model

A typical airfoil is viewed as a flat plate suspended from a fixed point by a spring. The basic model is illustrated in fig. 1, (York, 1980).

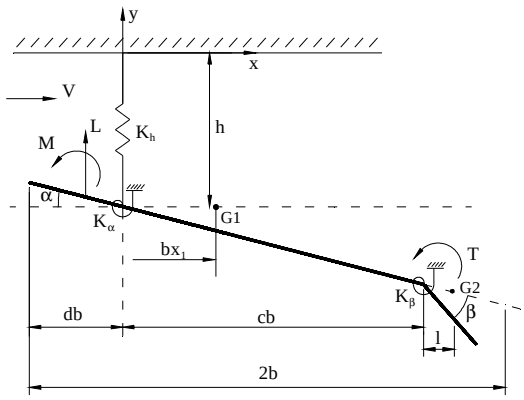

Figure 1. The 2-D cross-section of a typical airfoil.

The motion of the airfoil is described by three independent coordinates (degree of freedom): the plunge *h*, the pitch α, and the flap angle β. To provide the correct forces in order that the cross-section behaves like a part of the attached wing, one can use linear and torsional springs. The linear spring provides a restoring force for the plunge of the airfoil, and it is assumed to have constant stiffness K_h. Likewise, the torsional spring has constant stiffness K_α and the flap spring has constant stiffness K_β. The control flap is located at the trailing edge. The goal is to design a controller that produces an additional flap hing torque, T_s, used to control the flap.

The airfoil is subjected to three aerodynamic loads. The lift *L* is considered positive in the upward direction. The pitching moment *M* is assumed to be centered about the one-quarter chord of the airfoil. The flap torque *T* is applied to the flap hinge. A state space model is implemented that can be used for control design. Newton's second law and Euler equation ca be used to obtain the following equations of motion.

$$\sum_{i=1}^{2} F_y = m_i a_i \quad and \quad \sum_{i=1}^{2} M_{c.m.} = I_{Gi}\dot{\omega}_i \tag{1}$$

where *F* is force, *m* is mass, *i* is the number of rigid bodies, *a* is acceleration, *M* is momentum of external forces, *I* is the moment of inertia, and $\dot{\omega}$ is the angular acceleration. The subscript c.m. specifies that the variable is described in the center of mass. The free body diagram is shown in fig. 2, (Olds, 1997).

Equations (1) are applied to the main body (body 1) and to the trailing edge control surface (body 2). Small angles α and β are assumed, so the equations of motion can be linearized about the trivial equilibrium point. Equations (2-5) show this dynamic model, (considering $T_s = 0$):

$$K_h h - q_y + L_1 + m_1 \ddot{h} + m_1 b x_1 \ddot{\alpha} = 0 \tag{2}$$

$$I_{G1}\ddot{\alpha} + M_1 + K_\alpha \alpha - K_\beta \beta - K_h h b x_1 - L_1\left(db - \frac{b}{2} + b x_1\right) - q_y(cb - b x_1) = 0 \tag{3}$$

$$q_y + L_2 + m_2 \ddot{h} + m_2 bc\ddot{\alpha} + m_2 l\left(\ddot{\alpha} + \ddot{\beta}\right) = 0 \tag{4}$$

$$-\left(q_y + L_2\right)l + K_\beta \beta + M_2 + I_{G2}\left(\ddot{\alpha} + \ddot{\beta}\right) = 0 \tag{5}$$

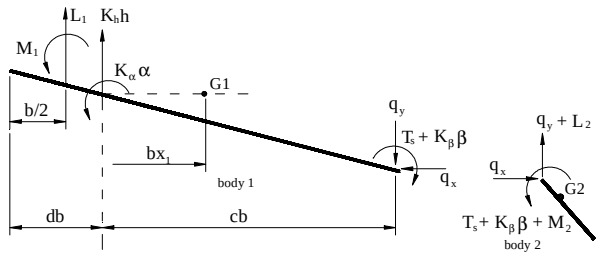

Figure 2. Free body diagram of the main body and trailing edge control surface.

Equations (2) and (3) are obtained from the main body and eqs. (4) e (5) from the trailing edge control surface. Here q_y is the vertical flap hinge force, q_x is the horizontal flap hinge force, l is the distance from the trailing edge flap to center of gravity from c, m_1 is the mass of body 1, m_2 is the mass of body 2, x_1 is the nondimensionalized distance of the main section center of gravity, I_{G1} is the moment of inertia per unit length of the total section, I_{G2} is the moment of inertia per unit span of trailing edge flap about point G_2, b is a normalizing constant, and c is the nondimensionalized distance to the flap hinge line.

After some mathematical manipulation, eqs. (2) to (5) can be combined in a second order system given by, (Olds, 1997):

$$\begin{bmatrix} bm & S_\alpha & S_\beta \\ bS_\alpha & I_\alpha & I_\beta + S_\beta cb \\ bS_\beta & I_\beta + S_\beta bc & I_\beta \end{bmatrix} \begin{Bmatrix} \ddot{h}/b \\ \ddot{\alpha} \\ \ddot{\beta} \end{Bmatrix} + \begin{bmatrix} bK_h & 0 & 0 \\ 0 & K_\alpha & 0 \\ 0 & 0 & K_\beta \end{bmatrix} \begin{Bmatrix} h/b \\ \alpha \\ \beta \end{Bmatrix} = \begin{Bmatrix} -L \\ -M \\ -(T + T_s) \end{Bmatrix} \tag{6}$$

where S_α is the static moment of the airfoil per unit length, S_β is the static moment of the control flap, I_α is the moment of inertia for the airfoil, and I_β is the moment of inertia for the control flap. The torque T_s is an additional flap hinge torque used to control the flap. The uncontrolled system is defined by $T_s = 0$. Equation. (6) can be written in the form:

$$M_a \ddot{Y}(t) + KY(t) = \begin{Bmatrix} -L \\ -M \\ -(T + T_s) \end{Bmatrix} \tag{7}$$

where:

$$\mathrm{M}_a = \begin{bmatrix} bm & S_\alpha & S_\beta \\ bS_\alpha & I_\alpha & I_\beta + S_\beta bc \\ bS_\beta & I_\beta + S_\beta bc & I_\beta \end{bmatrix} \tag{8}$$

and

$$K = \begin{bmatrix} bK_h & 0 & 0 \\ 0 & K_\alpha & 0 \\ 0 & 0 & K_\beta \end{bmatrix} \tag{9}$$

where M_a is the mass matrix and K is the stiffness matrix.

Following York (1980), equation (7) can be transformed to frequency domain and the motion of the airfoil is described by harmonic oscillations. Linearized equations and unsteady aerodynamic theory are considered. These considerations are applied to derive the motion equations, which give the pressure distribution over the wing and the aerodynamic responses of the oscillating hinges for any position of the hinge with respect to the leading edge. The linearization allows the total aerodynamic loads to be found by superposition of the forces and moments associated with each degree of freedom. Once the basic system has been derived, the inverse Fourier transform is used to construct a state space model. For more details about this topic see York (1980) and Olds (1997). For the present paper is considered the state space model of the form, (Bail, 1997):

$$\begin{aligned} \dot{x}(t) &= Ax(t) + Bu(t) \\ y(t) &= Cx(t) \end{aligned} \tag{10}$$

where A is the dynamic matrix, B is the input control matrix, C is the output matrix, $y(t)$ is the output vector, $u(t)$ is the input control (applied torque to the flap), and $x(t)$ is the state vector that is given by:

$$\begin{aligned} x(t) &= \left\{\dot{Y}(t) \quad Y(t) \quad x_a(t)\right\}^T, \quad Y(t) = \left\{h(t)/b \quad \alpha(t) \quad \beta(t)\right\}^T, \\ x_a(t) &= \left\{A_{a1}(t) \quad A_{a2}(t) \quad A_{a3}(t) \quad A_{a4}(t)\right\}^T \end{aligned} \tag{11}$$

where $x_a(t)$ are called aerodynamic-lag states, and it is used to describe the "states" of the fluid and to represent the aerodynamic load on the airfoil. The dynamic matrix A is 10 x 10; it has the form:

$$A = \begin{bmatrix} A_{11} & A_{12} & A_{13} \\ A_{21} & A_{22} & A_{23} \\ A_{31} & A_{32} & A_{33} \end{bmatrix} \tag{12}$$

where A_{ij} are derived in Olds (1997) and are given by:

$$A_{11} = -\left(M_a + \pi\rho b^2 Z_1\right)^{-1} \pi\rho b^2 Z_2 \tag{13}$$

$$A_{12} = -\left(M_a + \pi\rho b^2 Z_1\right)^{-1} \left(K + \pi\rho b^2 Z_3\right) \tag{14}$$

$$A_{13} = -\left(M_a + \pi\rho b^2 Z_1\right)^{-1} \pi\rho b^2 Z_4 \tag{15}$$

$$A_{21} = I_{3x3}, \quad A_{22} = 0_{3x3}, \quad A_{23} = 0_{3x4} \tag{16}$$

$$A_{31} = \begin{bmatrix} [R_1 \quad R_2 \quad R_3]A_{11} + [0 \quad R_4 \quad R_5] \\ [R_1 \quad R_2 \quad R_3]A_{11} + [0 \quad R_4 \quad R_5] \\ [R_6 \quad R_7 \quad R_8]A_{11} + [0 \quad R_9 \quad R_{10}] \\ [R_6 \quad R_7 \quad R_8]A_{11} + [0 \quad R_9 \quad R_{10}] \end{bmatrix} \tag{17}$$

$$A_{32} = \begin{bmatrix} [R_1 \quad R_2 \quad R_3]A_{12} \\ [R_1 \quad R_2 \quad R_3]A_{12} \\ [R_6 \quad R_7 \quad R_8]A_{12} \\ [R_6 \quad R_7 \quad R_8]A_{12} \end{bmatrix} \tag{18}$$

$$A_{33} = \begin{bmatrix} -\beta_1 V/b & 0 & 0 & 0 \\ 0 & -\beta_2 V/b & 0 & 0 \\ 0 & 0 & -\beta_1 V/b & 0 \\ 0 & 0 & 0 & -\beta_2 V/b \end{bmatrix} + \begin{bmatrix} [R_1 \quad R_2 \quad R_3]A_{13} \\ [R_1 \quad R_2 \quad R_3]A_{13} \\ [R_6 \quad R_7 \quad R_8]A_{13} \\ [R_6 \quad R_7 \quad R_8]A_{13} \end{bmatrix} \tag{19}$$

where ρ is the air density, Z_i ($i = 1,\ldots,4$) and $R_i (i = 1,\ldots,10)$ are constants, β_i ($i = 1,2$) are coefficients in exponent in two-term approximation to the Wagner function, and V is the velocity of the airfoil.

The R_i's constants are given in table 1,

Table 1. Ri's constants.

$R_1 = \frac{b^2}{V}$	$R_6 = \frac{b^2}{\pi V}\Phi_8$
$R_2 = \frac{b^2}{V}$	$R_7 = \frac{b^3}{\pi V}\Phi_8$
$R_3 = \frac{b^2}{2\pi V}$	$R_8 = \frac{b^3}{2\pi^2 V}\Phi_2\Phi_8$
$R_4 = V$	$R_9 = \frac{Vb}{\pi}\Phi_8$
$R_5 = \frac{V}{\pi}\Phi_1$	$R_{10} = \frac{Vb}{\pi^2}\Phi_1\Phi_8$

The Z_i's constants are given by, (Olds, 1997):

$$Z_1 = \begin{bmatrix} b & \frac{b}{2} & \frac{b}{2\pi}\Phi_4 \\ \frac{b^2}{2} & \frac{3b^2}{8} & \frac{b^2}{4\pi}\Phi_7 \\ \frac{b^2}{2\pi}\Phi_4 & \frac{b^2}{4\pi^2}\Phi_7 & \frac{b^2}{4\pi}\Phi_{12} \end{bmatrix} \tag{20}$$

$$Z_2 = \begin{bmatrix} 2V & 3V & \frac{V}{\pi}(\Phi_3 + \Phi_2) \\ 0 & Vb & \frac{Vb}{2\pi}\Phi_6 \\ \frac{Vb}{\pi}\Phi_8 & \frac{Vb}{\pi}\left(\frac{\Phi_9}{2} + \Phi_8\right) & \frac{Vb}{2\pi^2}(\Phi_1 + \Phi_2\Phi_8) \end{bmatrix} \tag{21}$$

$$Z_3 = \begin{bmatrix} 0 & \frac{2V^2}{b} & \frac{2V^2}{\pi b}\Phi_1 \\ 0 & 0 & \frac{V^2}{\pi}\Phi_5 \\ 0 & \frac{V^2}{\pi}\Phi_8 & \frac{V^2}{\pi^2}(\Phi_{10} + \Phi_1\Phi_8) \end{bmatrix} \tag{22}$$

$$Z_4 = \begin{bmatrix} \frac{-2V\alpha_1}{b} & \frac{-2V\alpha_2}{b} & 0 & 0 \\ 0 & 0 & 0 & 0 \\ 0 & 0 & \frac{-V\alpha_1}{b} & \frac{-V\alpha_2}{b} \end{bmatrix} \tag{23}$$

where $\Phi(V t/b)$ are Wagner functions (aerodynamic constants) that are derived in Olds (1997).

Now the input matrix B is given by:

$$B = \frac{1}{I_\beta}\begin{bmatrix} M_a^{-1}\begin{bmatrix} 0 \\ 0 \\ 1 \end{bmatrix} \\ 0 \\ 0 \\ 0 \\ 0 \\ 0 \\ 0 \end{bmatrix} \tag{24}$$

In this study, the measurements of plunge, pitch, the flap angle, and the respectives velocities are assumed to be measurable. So, the output matrix C is given by:

$$C = [I_{6x6} \quad 0_{6x4}] \tag{25}$$

Since a complete derivation of the model is not provided, once the aerodynamic-lag states are unmeasured, one must construct estimators for these states from the states that are measurable. The next section shows how to assure stability to closed-loop using LMI techniques to design a controller and a dynamic observer.

Observer-Based State-Feedback Control Solved by LMI

Rewriting eq. (10) and considering that the dynamic matrix has a parametric variation, so:

$$\begin{aligned} \dot{x}(t) &= A(t)x(t) + Bu(t), \quad A(t) \in \Omega \\ y(t) &= C\,x(t) \end{aligned} \tag{26}$$

where Ω is a polytope that is described by a list of vertexes in a convex space. The dynamic matrix is described by polytopic linear differential inclusion (LDI):

$$A(t) \in \Omega, \qquad \Omega = Co\{A_1, A_2, \cdots, A_v\} \tag{27}$$

where v is the number of vertexes of the polytopic system. The number of vertexes is givem by 2^p, where p is the number of uncertainty parameters. The operator Co means that the matrices A_1, A_2, …, A_v define a polyhedral convex bounded domain. A convex domain can have many different shapes, and Co precisely denotes the convex hull.

The problem to be investigated is state-feedback control, with the following linear control law:

$$u(t) = K_c x(t) \tag{28}$$

where K_c must be found. The system described by eq. (26) can be rewritten in closed-loop form:

$$\dot{x}(t) = (A(t) + BK_c)\, x(t), \quad A(t) \in \Omega \tag{29}$$

The system described by eq. (29) is quadratically stable if and only if there exists a symmetric matrix $Q=Q^T > 0$ such that:

$$Q(A_i + BK_c)^T + (A_i + BK_c)Q < 0 \tag{30}$$

where the symbols >0 and <0 means positive and negative definite, respectively, A_i is *ith* vertex of the polytopic system, i=1,2,..,v is the number of vertexes of the polytope.

Inequality (30) is not convex, because the condition is not jointly convex in K_c and Q. This constraint can be overcome by a simple trasformation of variables. We can obtain an equivalent LMI, defining $Y=K_cQ$:

$$QA_i^T + A_iQ + BY + Y^T B^T < 0, \quad i = 1,2,\cdots,v \tag{31}$$

which is an LMI in Q and Y. This LMI problem (LMIP) consists of finding $Q > 0$ and Y such that LMI (31) is feasible, or to determine if the LMI is infeasible, (Boyd et al., 1994). We can solve this LMIP by using interior-point methods, (Gahinet et al., 1995).

We can also impose a decay rate (or the largest Lyapunov exponent) to this problem. The decay rate is definied as the largest μ such that:

$$\lim_{t\to\infty} e^{\mu t} \| x(t) \| = 0 \tag{32}$$

holds for all trajectories of $x(t)$.

We can use the quadratic Lyapunov function, $V_{Lyap}(x)=x^TQ^{-1}x$, to establish a lower bound to the decay rate of the system. If $dV_{Lyap}(x)/dt \leq -2\mu V_{Lyap}(x)$ for all trajectories, then $V_{Lyap}(x(t)) \leq V_{Lyap}(x(0))e^{-2\mu t}$ and therefore the decay rate μ of the system is at least μ. These conditions are equivalent to the following LMIP:

$$QA_i^T + A_iQ + BY + Y^T B^T + 2\mu Q < 0, \quad i = 1,2,\cdots,v \tag{33}$$

When the initial condition is known, it is also possible to find an upper bound on the norm of the control input, eq. (28). Given $Q>0$ and Y, which satisfy the quadratic stabilization condition, the inequalities (33) are limited in the ellipsoid given by, (Folcher and Ghaoui, 1994):

$$\varepsilon = \left\{ x \in \Re^n \,\middle|\, x^T Q^{-1} x \leq 1 \right\} \tag{34}$$

The ellipsoid is said to be invariant if:

$$x(0) \in \varepsilon \Rightarrow \forall t > 0, \quad and \quad x(t) \in \varepsilon \tag{35}$$

where $x(0)$, the initial state, is given.

The upper bound of the control input can be written as:

$$\max_{t\geq 0} \|u(t)\| = \max_{t\geq 0} \left\| YQ^{-1}x(t) \right\| \leq \max_{x\in\varepsilon} \left\| YQ^{-1}x(t) \right\| = \\ = \lambda_{max}\left(Q^{-1/2} Y^T Y Q^{-1/2} \right)^{1/2} \tag{36}$$

where λ_{max} is the maximum eigenvalue of the following matrix $(Q^{-1/2}Y^TYQ^{-1/2})^{1/2}$.

Therefore, the constraints $\|u(t)\| < \sigma$ is enforced at all times $t>0$ if the LMIs below hold:

$$\begin{bmatrix} 1 & x(0)^T \\ x(0) & Q \end{bmatrix} \geq 0, \quad \begin{bmatrix} Q & Y^T \\ Y & \sigma^2 I \end{bmatrix} > 0 \tag{37}$$

where σ is the maximum value of input control amplitude.

The state-feedback gain matrix is $K_c = YQ^{-1}$, where Y and Q are solutions from LMIP (33) and (37). This problem can be solved using interior-point methods, (Gahinet et al., 1995). For each initial condition, the input u assure:

$$\forall t \geq 0, \quad \|u(t)\| < \sigma e^{-\mu t} \tag{38}$$

Since the aerodynamic-lag states are not measured it is essential to design a dynamic observer. In this work, it is considered the design of a deterministic observer to estimate the aerodynamic states that are not available. So, the input control is:

$$u(t) = K_c \bar{x}(t) \tag{39}$$

where $\bar{x}_c(t)$ is the estimated state vector. One can write the linear equation of the robust observer in the form, (Silva et al., 2004):

$$\dot{\bar{x}}(t) = A\bar{x}(t) + Bu(t) + K_e(C\bar{x}(t) - y(t)) \tag{40}$$

where K_e is the observer gain matrix, which can be obtained by different techniques. In the present work we have used LMI to obtain the observer gain matrix. It is possible to find an observer gain through the solution of the following LMI, (Boyd et al., 1994):

$$A^T P + PA + WC + C^T W^T + 2\gamma P < 0 \tag{41}$$

where γ is the decay rate of the observer, with $\gamma >> \mu$, and $P=P^T>0$ a symmetric matrix. To every P and W satisfying these LMI, there corresponds a stabilizing dynamic observer. The observer gain is given by $K_e = P^{-1}W$, where P and W are solutions to the LMI problem, as given by inequality (41).

The closed-loop system is given by:

$$\begin{Bmatrix} \dot{x}(t) \\ \dot{\bar{x}}(t) \end{Bmatrix} = \begin{bmatrix} A & BK_c \\ -K_eC & A + K_eC + BK_c \end{bmatrix} \begin{Bmatrix} x(t) \\ \bar{x}(t) \end{Bmatrix} \tag{42}$$

Open-Loop Simulations

To verify the proposed methodology, the results of simulations of an open-loop system for diferentes flow velocities are presented. We consider the following velocities $V = 290$ m/s, $V = 298$ m/s and $V = 305$ m/s. The velocity $V = 298$ m/s is the flutter velocity (V_f). It represents the velocity for which the open-loop system becomes

marginally stable. So, for $V < V_f$ the system is asymptotically stable and for $V > V_f$ the system is unstable. In this case, the airfoil would become unstable and wing separation would occur. It is a dangerous situation in a real system.

Figures 3, 4 and 5 show the aerolastic time response for each flow velocity without considering uncertainty in any parameter. The list of constants are given in table 2. We considered, for these numerical applications, the following initial condition vector:

$$x(0) = \begin{Bmatrix} 0.0152 \\ -0.01 \\ 0.005 \\ -0.003 \\ 0.0001 \\ 0.0001 \\ 0 \\ 0 \\ 0 \\ 0 \end{Bmatrix} \tag{43}$$

Table 2. List of Constants

Parameter	Value (International System)
α_1	*0.0165*
α_2	*0.335*
b	*0.914* [m]
β_1	*0.41*
β_2	*0.32*
c	*1.0*
I_α	*2.69e1* [kg.m]
I_β	*6.73e-1* [kg.m]
m	*1.287e2* [kg/m]
K_h	$m*50^2$ [N/m]
K_α	$I_\alpha 100^2$ [N/m]
K_β	$I_\beta 500^2$ [N/m]
ρ	*1225* [kg/m^3]
S_α	*2.35e1* [kg]
S_β	*1470* [kg]

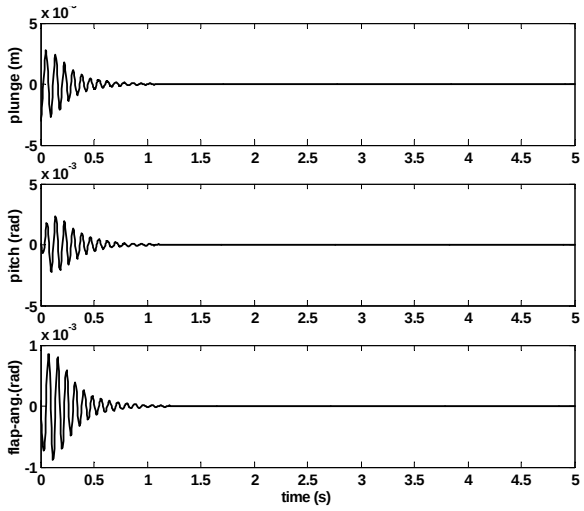

Figure 3. Aeroelastic time response to initial condition in open-loop, considering V = 290 m/s < Vf, (stable system, V < Vf).

Closed-Loop Simulations

This section is devoted to the controller design for the flow velocity $V = 305$ m/s (unstable case). The goal is to design an LMI regulator based on the solution of inequalities (33) and (37) for the controller and inequalities (41) for the observer. The values $\mu = 1$, $\gamma = 3$ and $\sigma = 250$ were chosen in order to represent practical values for constrains.

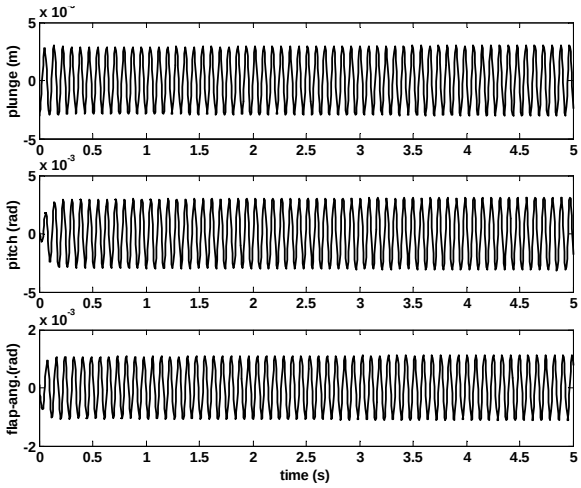

Figure 4. Aeroelastic time response to initial condition in open-loop, considering V = V_f = 298 m/s, (marginally stable system).

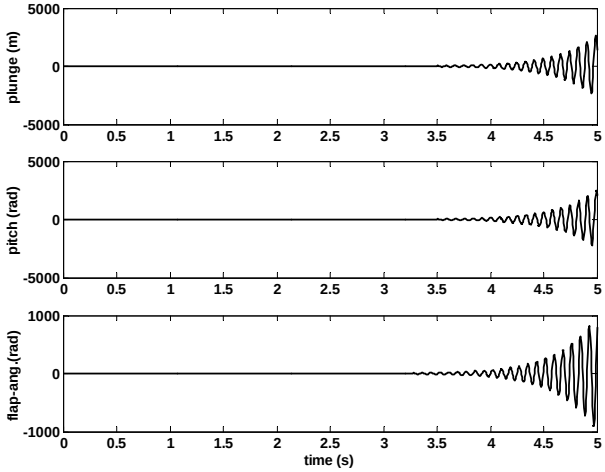

Figure 5. Aeroelastic time response to initial condition in open-loop, considering V = 305 m/s > V_f , (unstable system, V > V_f).

First the regulator is designed non-robust for uncertainties. The non-robust state-feedback gain matrix is obtained by solving the following LMIP:

$$\begin{aligned} &Q > 0 \\ &QA^T + AQ + BY + Y^T B^T + 2\mu Q < 0 \\ &\begin{bmatrix} 1 & x(0)^T \\ x(0) & Q \end{bmatrix} \geq 0 \\ &\begin{bmatrix} Q & Y^T \\ Y & \sigma^2 I \end{bmatrix} > 0 \end{aligned} \tag{44}$$

The gain matrix $K_c=YQ^{-1}$ is reached by solving inequalities (44). The non-robust observer gain matrix is obtained by $K_e=P^{-1}W$, where P and W are solutions to LMIP given by:

$$P > 0, \qquad A^T P + PA + WC + C^T W^T + 2\gamma P < 0 \tag{45}$$

Figure 6 shows the closed-loop response for this condition. The controller reached the requirements and the closed-loop simulation obtained is stable. The input control for this robust regulator, an additional flap hing torque, T_s, is computed by using eq. (39), figure 7.

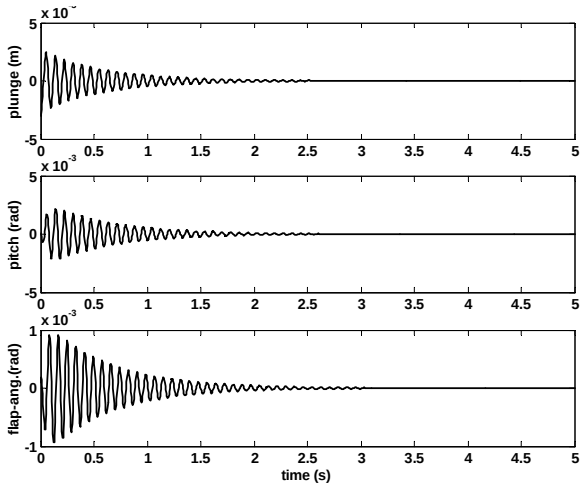

Figure 6. Aeroelastic time response to initial condition in closed-loop, considering V = 305 m/s > V_f , stable system (non-robust regulator).

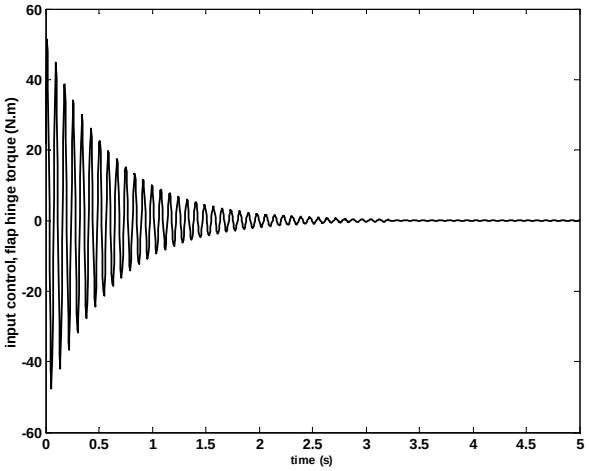

Figure 7. Input control (additional flap hing torque, T_s) considering the systen in nominal condition (non-robust regulator).

However, when considering a parametric variation, it was found that the closed-loop system became unstable. The system was assumed to have a possible variation of ± 10 % in the values of stiffness of the flap spring (K_β), stiffness of pitch (K_α) and stiffness of plunge (K_h). So, it has three uncertainty parameters ($p=3$):

$$\begin{aligned} K_\beta^{\min} &= 0.9K_\beta^{N} < K_\beta < K_\beta^{\max} = 1.1K_\beta^{N} \\ K_\alpha^{\min} &= 0.9K_\alpha^{N} < K_\alpha < K_\alpha^{\max} = 1.1K_\alpha^{N} \\ K_h^{\min} &= 0.9K_h^{N} < K_h < K_h^{\max} = 1.1K_h^{N} \end{aligned} \tag{46}$$

where K_β^N, K_α^N and K_h^N are the nominal values of parameters of the respectives springs. For the above consideration, there are eight (2^3) vertexes of the polytopic system. The uncertainties are shown in figure 8. The vertexes of the parameter box are a combination of the minimum and maximum values of uncertainties of the system. It is supposed that the system can assume any combination of values inside the box. The vertexes correspond to V1 (K_β^{min}, K_α^{min}, K_h^{min}), V2 (K_β^{min}, K_α^{max}, K_h^{min}), V3 (K_β^{min}, K_α^{min}, K_h^{max}), V4 (K_β^{min}, K_α^{max}, K_h^{max}), V5 (K_β^{max}, K_α^{min}, K_h^{min}), V6 (K_β^{max}, K_α^{max}, K_h^{min}), V7 (K_β^{max}, $K_\alpha^{m,in}$, K_h^{max}), and V8 (K_β^{max}, K_α^{max}, K_h^{max}). These vertexes define the possible dynamic matrices A_1, A_2, … and A_8.

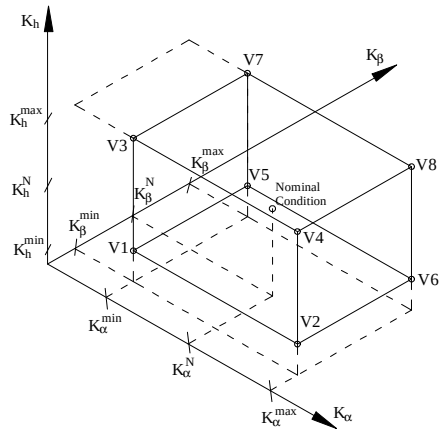

Figure 8. Parameter box showing the uncertainties combinations.

The non-robust regulator, designed by LMIPs (44) and (45), assures only the requirements to system in the nominal condition.

In order to test the system, the condition of vertexes V5 and V7 was considered. Figures 9 and 10 present the time responses of the closed-loop considering the system in vertexes V5 and V7, respectively. Clearly, this regulator is not robust to uncertainties in the considered parameters. The results were similar for all other vertexes tested.

So, it is required to design an LMI regulator to assure quadratic stability in the closed-loop considering parametric variation of the springs. To solve this problem, the model with parametric uncertainties can be quantified by ranges of parameter values. The parameters uncertainties ranges can be described as a parameter box, shown in figure 8. The controller that satisfies all systems described inside this convex space is said to be robust to parametric variations. In order to satisfy this requirement it is enough to solve the LMI problems from inequalities (33), (37) and (41) for all eight vertexes simultaneously. The controller can be found using the following LMIs:

$$
\begin{gathered}
QA_1^T + A_1Q + BY + Y^TB^T + 2\mu Q < 0 \\
QA_2^T + A_2Q + BY + Y^TB^T + 2\mu Q < 0 \\
\vdots \\
QA_8^T + A_8Q + BY + Y^TB^T + 2\mu Q < 0 \qquad (47) \\
Q > 0 \\
\begin{bmatrix} 1 & x(0)^T \\ x(0) & Q \end{bmatrix} \geq 0 \\
\begin{bmatrix} Q & Y^T \\ Y & \sigma^2 I \end{bmatrix} > 0
\end{gathered}
$$

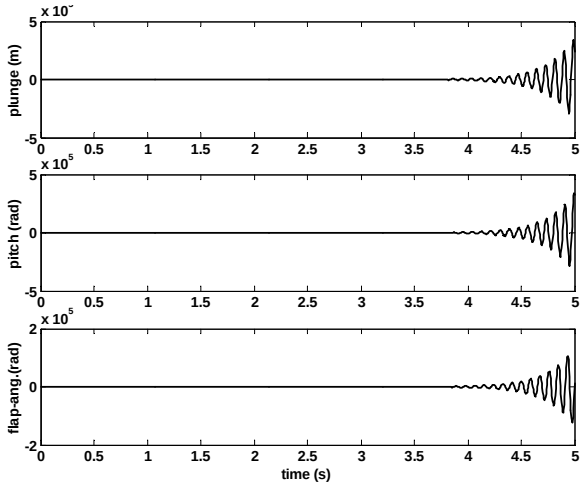

Figure 9. Aeroelastic time response in closed-loop considering condition of vertex V5, unstable system (non-robust regulator).

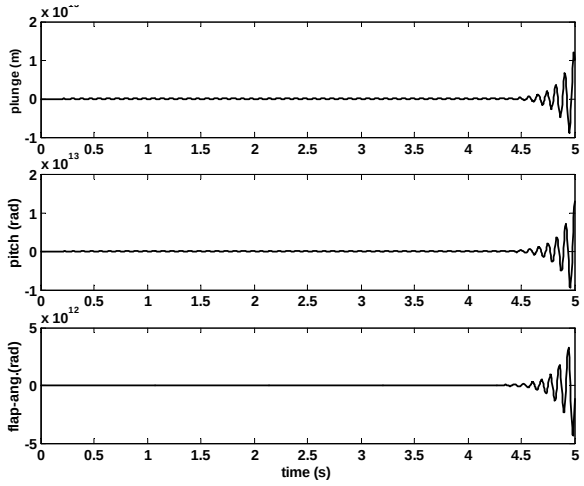

Figure 10. Aeroelastic time response in closed-loop considering condition of vertex V7, unstable system (non-robust regulator).

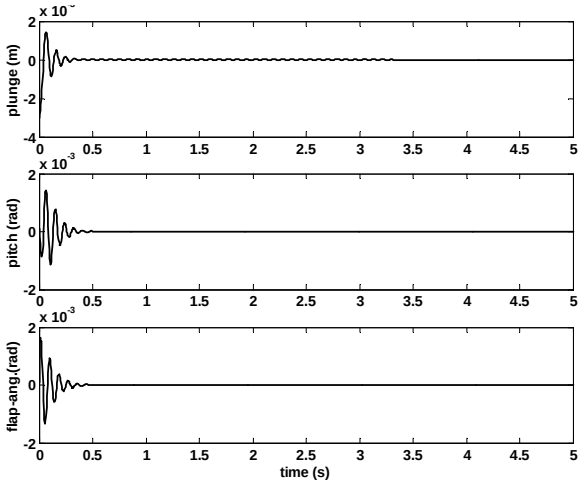

Figure 11. Aeroelastic time response in closed-loop considering condition of vertex V1 and V > Vf (robust regulator).

The robust state-feedback gain matrix is $K_c=YQ^{-1}$, where Y and Q are solutions to LMIP (47), where $x(0)$, σ and μ are known. The observer gain matrix is obtained by $K_e=P^{-1}W$, where P and W are solutions to LMIP given by inequality (45).

Figures 11, 12, 13 and 14 show the time responses to initial condition considering the robust controller to vertexes V1, V5, V7 and V8 for $V = 305$ m/s ($V>V_f$). The results of all other vertexes were similar.

Analysing figures 11, 12, 13 and 14 it is possible to conclude that the regulator is robust to the considered parametric variations. However, nothing can be said about variation in other parameters. For any other parameter variation the procedure is the same, and it is necessary to consider all vertexes in a polytopic system.

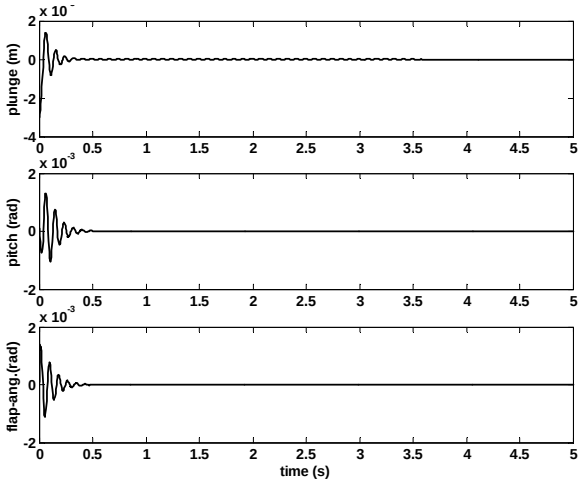

Figure 12. Aeroelastic time response in closed-loop considering condition of vertex V5 and V > Vf (robust regulator).

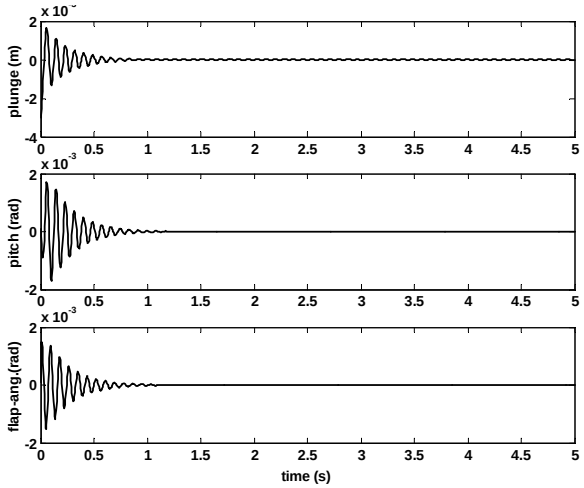

Figure 13. Aeroelastic time response in closed-loop considering condition of vertex V7 and V > Vf (robust regulator).

Figure 15 shows the aeroelastic time response considering the system in the nominal condition (K_β^N, K_α^N, K_h^N). The controller designed satisfied the requirements and the closed-loop obtained was stable when feedback with robust regulator.

The input control to the robust regulator (additional flap hing torque, T_s) is computed by using equation (39). Figure 16 shows T_s considering the system in the nominal conditions. For the other conditions inside the uncertainty combinations the responses were similar.

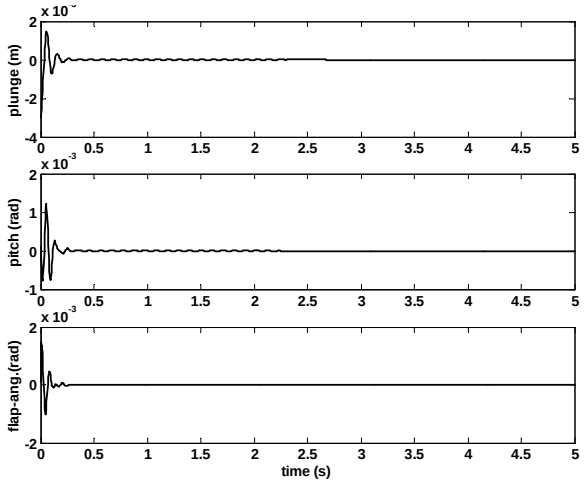

Figure 14. Aeroelastic time response in closed-loop considering condition of vertex V8 and V > Vf (robust regulator).

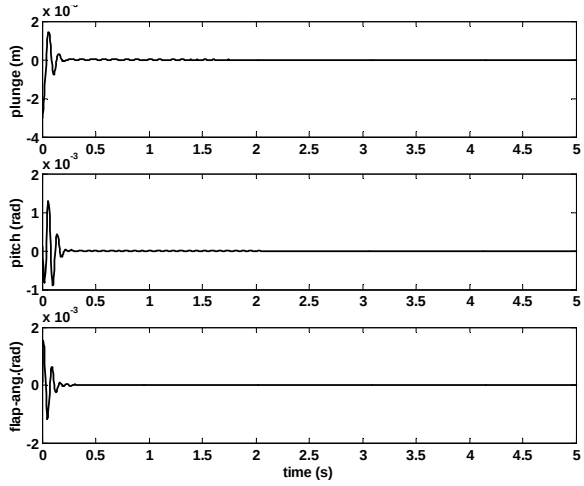

Figure 15. Aeroelastic time response to initial condition in closed-loop, considering nominal condition, stable system (robust regulator).

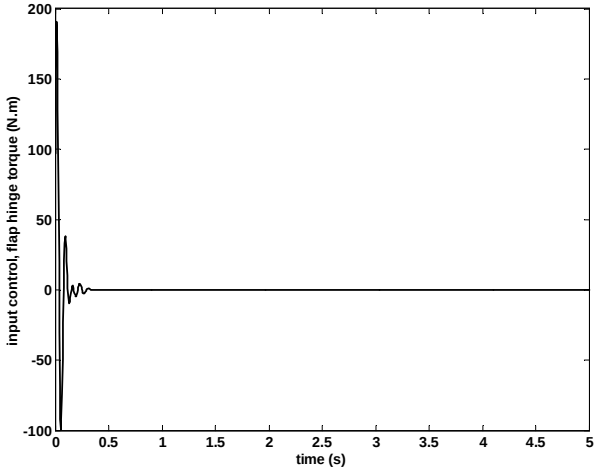

Figure 16. Input control (additional flap hing torque, Ts) considering the system in nominal condition (robust regulator).

Conclusions

In this paper an alternative solution to suppress fluter in a 2-D airfoil by using active control were presented. We have chosen to use LMI techniques due to some advantages when compared with other techniques, as for instance, the facility to solve robust problems and formulation well defined in literature, (Boyd et al., 1994).

In the first part of this paper, a brief review was made of linear classical aeroelastic 2D-airfoil model and the state space realization. Following this, the strategy to design the regulator (controller and observer) was discussed. The proposal methodology was verified through two different designs of regulator, the first one is a non-robust to parametric variation and the other one is a robust design. The results showed that the system becomes unstable under feedback control with the non-robust regulator for parametric variation in the spring constants of the system. On the other hand, with robust regulator design the system was kept stable for flutter velocity conditions.

As a further study, we propose to use fuzzy Takagi-Sugeno models based on an LMI design to develop a non-linear regulator to suppress flutter in aircraft. So, in this case, it is possible to consider

several non-linearities omited in the model used in this work or still to use a more advanced model. This kind of control design is well defined in literature and has many successful citations, as for instance, Tanaka et al. (1998) and Teixeira et al. (2001).

Acknowledgements

The authors acknowledge the support of the Research Foundation of the State of São Paulo (FAPESP-Brazil). The authors would also like to thank the Associate Editor and reviewers for the valuable comments.

References

Bail, T. R., 1997, "A Disturbance-Rejection Problem For A 2-D Airfoil", MS thesis, Virginia Polytechnic Institute and State University.

Belo, E. M., Rocha, J. C. and De Marqui Jr., C., 2001, "A Fuzzy Controller for Active Flutter Suppression", Proceedings of 9th International Symposium on Dynamic Problems of Mechanics, Florianópolis/SC, Brazil, pp. 9- 14.

Bisplinghoff, R. L., Ashley, H., Halfman, R. L., 1996, "Aeroelasticity", Addison-Wesley Publishing Company, USA.

Boyd, S., Balakrishnan, V., Feron, E. and El Ghaoui, L, 1993, "Control System Analysis and Synthesis via Linear Matrix Inequalities", Proceeding of American Control Conference, pp. 2147-2154.

Boyd, S., Balakrishnan, V., Feron, E. and El Ghaoui, L, 1994, Linear Matrix Inequalities in Systems and Control Theory, SIAM Studies in Applied Mathematics, USA.

De Marqui Jr., C., Benini, G. R. and Belo, E. M., 2001, "Uma Revisão Histórica do Fenômeno Flutter", Proceedings of 16th Brazilian Congress of Mechanical Engineering, Uberlândia/MG, Brazil, (CD-Room).

Folcher, J. P. and Ghaoui, L., 1994, "State-Feedback Design via Linear Matrix Inequalities Application to a Benchmark Problem", IEEE ISBN 0-7803-1872-2, pp. 1217-1222.

Gahinet., P., Nemirovski, A.,. Laub, A. J. and Chiliali, M., 1995, LMI Control Toolbox User's Guide, The Mathworks Inc., Natick, MA, USA.

Garrick, I. E., 1976, "Aerolasticity – Frontiers and Beyond", Journal of Aircraft, v. 13, n. 9, p. 641-657.

Ghaoui, L. and Niculescu, S., 2000, Advances in Linear Matrix Inequalities Methods in Control. Siam, USA.

Geromel, J. C., Peres, P. L. D. and Bernussou, J., 1991, "On a Convex Parameter Space Method for Linear Control Design of Uncertain Systems", SIAM J. Control and Optimization, 29 (2), pp. 381-402.

Haley, P. and Soloway, D., 1996, "Experimental Validation of Generalized Predictive Control for Active Flutter Suppression", In: Proceedings of the IEEE International Conference on Control Applications, p. 125-129.

Harman, D. and Liu, H. H. T, 2002, "Robust Flight Control: A Real-Time Simulation Investigation", Proceedings of the 23rd International Congress of Aeronautical Sciences (ICAS), Toronto, Canada, September 8-13, 2002, ICAS 2002-5.4.3.

Lewis, F. L., Jagannathan, S. and Yesildirek, A., 1999, "Neural Network Control of Robot Manipulators and Nonlinear Systems", Taylor & Francis, 441p.

Norlander, T., Nilsson, B., Ring, D. and Johansson, U., 2000, "A Study On Active Flutter Detection And Control", 0-7803-6262-4/00, IEEE, pp. 172-179.

Olds, S., 1997, "Modelling and LQR Control of a Two-Dimensional Airfoil", MS thesis, Virginia Polytechnic Institute and State University.

Oliveira, M. C., Farias, D. P. and Geromel, J. C., 1997, "LMISol, User's Guide", UNICAMP, Campinas-SP, Brasil.

Silva, S., Lopes Jr, V. and Assunção, E., 2004, "Robust Control of Truss Structure Using Linear Matrix Inequalities", in proceedings of the XXII IMAC – Conference & Exposition on Structural Dynamics, Dearborn, Michigan, USA.

Tanaka, K., Ikeda, T. and Wang, H. O. , 1998, "Fuzzy Regulators and Fuzzy Observers: Relaxed Stability Conditions and LMI-Based Designs". IEEE Transactions on Fuzzy Systems. v. 6, n. 2, p. 250-265.

Teixeira, M. C. M., Avellar, R. G. and Assunção, E, 2001, "On Relaxed LMI-Based Design for Fuzzy Controllers". Melbourne. In: Proceedings of the 2001 IEEE International Conference on Fuzzy Systems, p. 704-707. Dec. 2001.

York, D. L., 1980, "Analysis of Flutter Suppression via An Energy Method", MS thesis, Virginia Polytechnic Institute and State University.